

PACS numbers: 07.60.Vg; 42.81.–i; 42.40.Eq
DOI: 10.1070/QE2006v036n10ABEH013190

Simple method for apodization of fibre Bragg gratings written by a Gaussian beam

S.R. Abdullina, S.A. Babin, A.A. Vlasov, S.I. Kablukov

***Abstract*. The possibilities of apodization of fibre Bragg gratings written by the holographic method with a Gaussian beam are considered. A simple method is demonstrated for smoothing the spectral profile of highly reflecting gratings by illuminating the written interference pattern by a homogeneous Gaussian beam.**

Keywords: *fibre Bragg grating, apodization, interference, reflection spectrum.*

1. Introduction

Fibre Bragg gratings (FBGs) show considerable promise for the use in telecommunication and sensor systems and are a key element of fibre lasers [1, 2]. Wide applications of FBGs are determined by their unique spectral properties, all-fibre structure, and low losses introduced by them. The modern manufacturing technology of FBGs allows their applications in industry and technology.

A fibre Bragg grating is an optical fibre with a periodic variation in the refractive index in the fibre core. Such a structure is formed by modifying the core glass by UV light with a spatially modulated intensity which can be produced, for example, due to the interference of two laser beams [3]. The relative change $\Delta n/n$ in the refractive index can achieve $\sim 10^{-2}$ [4]. The FBG spectrum has the resonance nature due to the constructive interference of waves reflected from layers with different refractive indices. The reflection coefficient is maximal near the so-called Bragg wavelength $\lambda_{\mathrm{Br}} = 2n\Lambda$, where n is the effective refractive index of the optical fibre and Λ is the modulation period. Due to reflections at the FBG ends, the effective Fabry–Perot resonator is formed, resulting in the appearance of side resonances in the spectrum.

The intensity of side resonances in the spectra of highly reflecting gratings can be several per cent and more, which is inadmissible for some applications. The side resonances are suppressed by using the so-called apodization of gratings [1, 2, 5, 6] which provides a continuous variation in the amplitude of the induced refractive index along the FBG, resulting in a decrease in the influence of a finite length of the FBG on the reflection spectrum. There exist numerous profiles $\Delta n(z)$ of the induced refractive index providing the suppression of side resonances in the FBG spectrum [1]. However, the realisation of most of them in practice requires technologically complicated scanning methods.

The aim of our paper was to study the possibility of writing highly reflecting FBGs with a smooth reflection profile without scanning by using a typical Gaussian laser beam. A specific feature of the method proposed is the FBG apodization procedure that does not require any transformation of the UV laser beam. Being relatively simple, this method is quite efficient and provides the suppression of side resonances down to -20 dB.

S.R. Abdullina, S.A. Babin, A.A. Vlasov, S.I. Kablukov Institute of Automation and Electrometry, Siberian Branch, Russian Academy of Sciences, prosp. akad. Koptyuga 1, 630090 Novosibirsk, Russia; e-mail: babin@iae.nsk.su

Received 18 April 2006; revision received 15 June 2006
Kvantovaya Elektronika **36** (10) 966–970 (2006)
Translated by M.N. Sapozhnikov

2. Basic expressions

The shape of the FBG spectrum is determined by a variation in the refractive index along a fibre:

$$n(z) = n_0 + \Delta n(z) = n_0 + \Delta n_{\mathrm{dc}}(z) + \Delta n_{\mathrm{ac}}(z)\cos\left(\frac{2\pi}{\Lambda}z\right), \quad (1)$$

where n_0 is the effective refractive index of the optical fibre; $\Delta n_{\mathrm{dc}}(z)$ is the average value of the UV laser-induced refractive index; and $\Delta n_{\mathrm{ac}}(z)$ is the modulation amplitude. In the case of interference FBG writing schemes for a linear dependence of the induced refractive index on the UV radiation dose, the relation $\Delta n_{\mathrm{ac}}(z) = s\Delta n_{\mathrm{dc}}(z)$ is fulfilled, where s is the visibility of the interference pattern. For a FBG with the homogeneous refractive index profile, i.e. a constant variation in the refractive index amplitude over the fibre length $\Delta n_{\mathrm{ac}}(z) = \mathrm{const}$, the reflection spectrum can be found analytically [1]. The maximum reflection coefficient is

$$R = \tanh^2\left[\pi\frac{\Delta n_{\mathrm{ac}}}{2(n_0 + \Delta n_{\mathrm{dc}})\Lambda}L\right]. \quad (2)$$

The relative width of the spectrum defined as the distance between the first zeroes in the reflection spectrum normalised to the wavelength is

$$\frac{\Delta\lambda}{\lambda} = \left[\left(\frac{\Delta n_{\mathrm{ac}}}{n_0}\right)^2 + \left(\frac{2\Lambda}{L}\right)^2\right]^{1/2}. \quad (3)$$

The side resonances in the FBG spectrum of this type are intense and achieve a few tens of per cent in highly reflecting ($R \sim 1$) gratings [1].

In the case of the interference of Gaussian beams,

$$\Delta n_{\rm dc}(z) = \Delta n_0 \exp\left(-\frac{2z^2}{w^2}\right), \quad \Delta n_{\rm ac}(z) = s\Delta n_0 \exp\left(-\frac{2z^2}{w^2}\right),$$

$$\Delta n(z) = \Delta n_0 \exp\left(-\frac{2z^2}{w^2}\right)\left[1 + s\cos\left(\frac{2\pi}{\Lambda}z\right)\right], \qquad (4)$$

where w is the radius of a Gaussian beam. In this case, the Bragg wavelength $\lambda_{\rm Br} = 2n\Lambda$ is maximal at the grating centre, where $n(z=0) = n_0 + \Delta n_0$ and decreases towards its edges. Therefore, the edge regions can form the effective Fabry–Perot resonator producing side resonances in the short-wavelength region of the spectrum of highly reflecting FBGs [7]. To eliminate this effect, it is necessary to provide a constant average value of the induced refractive index along the FBG, $\Delta n_{\rm dc} = \text{const}$ [1, 2, 6]. In this case,

$$\Delta n(z) = \Delta n_0 \exp\left(-\frac{2z^2}{w^2}\right)\left[1 + s\cos\left(\frac{2\pi}{\Lambda}z\right)\right]$$

$$+ \Delta n_0\left[1 - \exp\left(-\frac{2z^2}{w^2}\right)\right]$$

$$= \Delta n_0 s \exp\left(-\frac{2z^2}{w^2}\right)\cos\left(\frac{2\pi}{\Lambda}z\right) + \Delta n_0, \qquad (5)$$

and the amplitude of side resonances can be reduced down to -30 dB [6]. However, such a complicated beam profile (a constant intensity with a Gaussian hole) can be produced only by using a special amplitude mask or the scanning method. In this paper, we consider the possibility of obtaining the homogeneous distribution of the average refractive index by using a Gaussian beam both for writing a periodic structure and apodization. We show that the homogeneous illumination of an optical fibre by a Gaussian beam at points z_1 to the right and $-z_2$ to the left of the FBG centre with the Gaussian envelope

$$\Delta n(z) = \Delta n_0 \exp\left(-\frac{2z^2}{w^2}\right)\left[1 + s\cos\left(\frac{2\pi}{\Lambda}z\right)\right]$$

$$+ \Delta n_1 \exp\left[-\frac{2(z-z_1)^2}{w^2}\right] + \Delta n_2 \exp\left[-\frac{2(z+z_2)^2}{w^2}\right] \qquad (6)$$

provides a constant average value of the refractive index along the FBG at the interval from $-w$ to w with an accuracy of $\sim 10\,\%$ for $z_1 \approx z_2 \approx w$ and $\Delta n_1 \approx \Delta n_2 \approx \Delta n_0$.

3. Experiment

We fabricated earlier a high-power coherent UV radiation source for the use in interferometric FBG writing schemes [8]. The intracavity frequency doubling of an argon laser ($\lambda = 488$ nm) with a wide-aperture gas-discharge tube gave up to 1 W of cw UV radiation power (with the coherence length of ~ 5 cm), which is optimal for FBG writing in the maximum absorption region (at $\lambda \sim 240$ nm) in germanium-doped optical fibres. Frequency doubling was performed in a nonlinear BBO crystal.

Figure 1 presents our interferometric scheme. Radiation from UV laser (*1*) passes through phase mask (*4*) and is incident on a fibre without a protective polymer jacket, which is placed close to the phase mask, i.e. in the region of interference of the waves diffracted to the $+1$ and -1 orders of the phase mask. The profile of phase mask grooves provides the suppression of the zero diffraction order down to 7 % and the localisation of $\sim 75\,\%$ of energy in the $+1$ and -1 orders (which corresponds in the first approximation to the visibility of the interference pattern $s = 0.75$). Cylindrical lens (*3*) focuses radiation along the fibre, providing the increase in the radiation intensity to ~ 100 W cm^{-2}. All experiments were performed under nearly the same conditions. Beam expander (*2*) is used to vary the illumination region along the fibre. Spectral characteristics are recorded with optical spectrum analyser (*5*) with a resolution of 0.017 nm and broadband LED (*7*). The reflection spectra are recorded by using additionally circulator (*6*) providing the unidirectional transmission from port I to II and from port II to III.

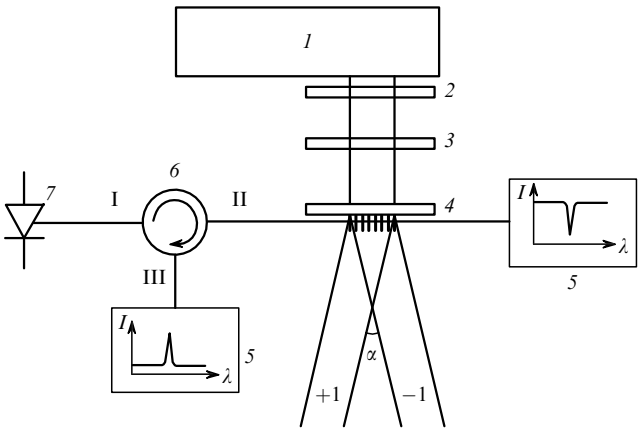

Figure 1. Scheme of the experiment: (*1*) UV laser; (*2*) beam expander; (*3*) cylindrical lens; (*4*) phase mask; (*5*) optical spectrum analyser; (*6*) circulator; (*7*) LED; (I, II, III) ports.

We used an AllWave™ fibre in experiments. The photosensitivity of the fibre was increased by keeping it preliminary in the hydrogen atmosphere at a pressure of 100 atm for ~ 10 days [4].

We performed a series of experiments on FBG writing by a Gaussian beam of radius $w = 3.5 \pm 0.4$ and 1.1 ± 0.2 mm. Figures 2 and 3 show the FBG reflection spectra obtained after different exposure times. During FBG writing, the resonance peak shifted to the red and broadened. At a certain stage, side resonances appeared in the short-wavelength region of the spectrum. The spectrum of a long FBG was narrower than that of a short one, in accordance with expression (3).

Figure 4 shows the dependence of a variation $\Delta n_{\rm dc}$ in the induced refractive index on the exposure time determined from the approximation of experimental spectra by theoretical curves calculated numerically, which corresponds to the change in the resonance FBG wavelength $\lambda_{\rm Br} = 2(n_0 + \Delta n_{\rm dc})\Lambda$. The FBG writing dynamics is well studied and corresponds in our case to the commonly known dynamics [1, 2]. Under our experimental conditions, the induced refractive index in the first approximation changed linearly with increasing the irradiation dose, which is proportional to the exposure time at a fixed UV laser power.

By using the interference of Gaussian beams for FBG writing, we obtained the spectrum with the side resonance

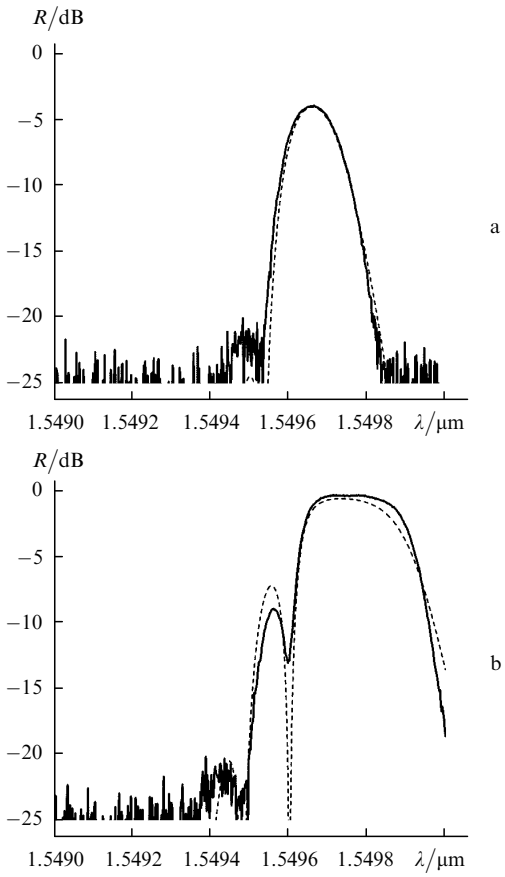

Figure 2. Dependences of the reflection coefficient R on the wavelength λ for the FBG for $w = 3.5 \pm 0.4$ mm and the exposure time 52 (a) and 120 s (b). The dashed curves are numerical simulations of the spectrum of the FBG described by expression (4) for $w = 3.89$ mm, $s = 0.75$, $n_0\Lambda = 0.7748$ μm, $\Delta n_0 = 0.1 \times 10^{-3}$ (a) and 0.27×10^{-3} (b).

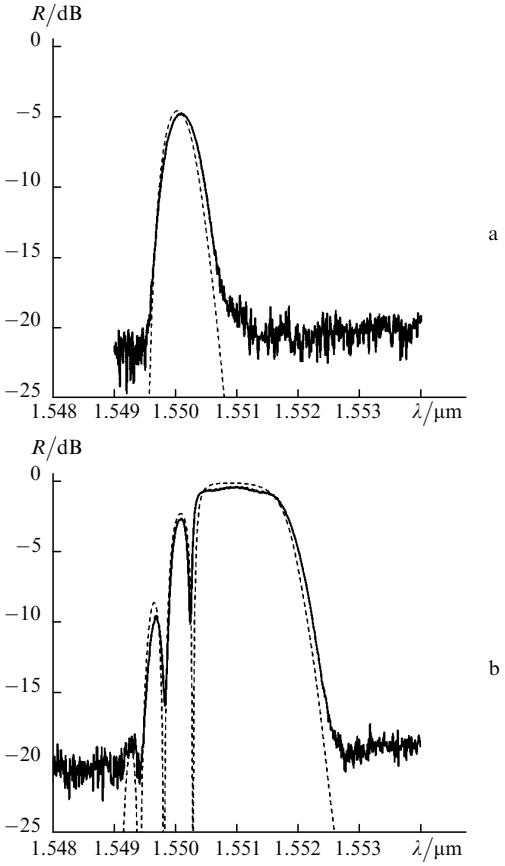

Figure 3. Dependences of the reflection coefficient R on the wavelength λ for the FBG for $w = 1.1 \pm 0.2$ mm and the exposure time 15 (a) and 100 s (b). The dashed curves are numerical simulations of the spectrum of the FBG described by expression (4) for $w = 1$ mm, $s = 0.75$, $n_0\Lambda = 0.7748$ μm, $\Delta n_0 = 0.37 \times 10^{-3}$ (a) and 1.6×10^{-3} (b).

amplitude less than −20 dB, the reflection coefficient up to 30 %, and the −3-dB level width from ∼0.138 nm (Fig. 2a) to ∼0.58 nm (Fig. 3a). As the reflection coefficient was increased, the side resonances appeared due to the interference effect (Figs 2b and 3b). They were suppressed by using homogeneous illumination to flatten the average value of the induced refractive index along the FBG. For this purpose, according to (6), after FBG writing by the UV Gaussian beam of radius $w = 1.1 \pm 0.2$ mm, the fibre was displaced to the right and left by a distance of 1 mm (close to the beam radius) and was illuminated by the same beam during approximately the same time, but already without the phase mask. Figure 5 presents the initial FBG spectrum and the FBG spectrum after the amplitude illumination by the Gaussian beam; the insets show the corresponding refractive index profiles. We obtained by this method the spectrum of a highly reflecting grating with side resonance suppressed down to the level no more than −20 dB, which was determined by the sensitivity of our detection equipment.

4. Numerical simulation

We compared our experimental results with numerically simulated FBG spectra.

Consider the initial equations. It is known that the propagation of a one-dimensional scalar monochromatic wave in a medium is described by the wave equation [9]

$$\frac{\mathrm{d}^2E}{\mathrm{d}z^2} + k^2E = 0, \tag{7}$$

where $E = E(z)$ is the scalar field, more exactly – one of the components of the electromagnetic field vector; $k = k_0 n(z)$; k_0 is the wave number of the light wave in vacuum; and n is the specified refractive index of the medium.

We considered the problem of scattering (partial reflection) of a wave with the unit amplitude incident from the left on an inhomogeneous region – the interval $(-L/2, L/2)$. In this case, the field E for $z \leqslant -L/2$ is represented in the form

$$E = A_1 \exp(\mathrm{i}k_1 z) + B_1 \exp(-\mathrm{i}k_1 z),$$

where A_1 and B_1 are the complex amplitudes of the incident and reflected waves, respectively; $k_1 = k_0 n_0$ is the wave number; and

$$|A_1| = 1. \tag{8}$$

For $z \geqslant L/2$, only the transmitted wave $E = A_2 \exp(\mathrm{i}k_1 z)$ with the complex amplitude A_2 is present. The field E inside the interval $(-L/2, L/2)$ and amplitudes A_2 and B_1 were determined by solving numerically Eqn (7). Due to the linearity of Eqn (7), we can specify the initial conditions at the right boundary, solve the equation, and then multiply the obtained solution by a coefficient K_c to satisfy condition

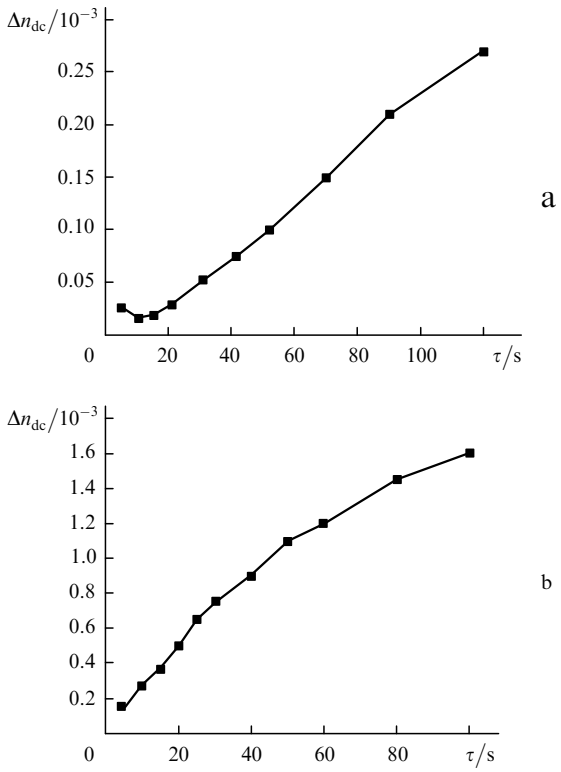

Figure 4. Dependences of the induced refractive index Δn_{dc} on the exposure time τ for the FBG for $w = 3.5 \pm 0.4$ (a) and 1.1 ± 0.2 mm (b).

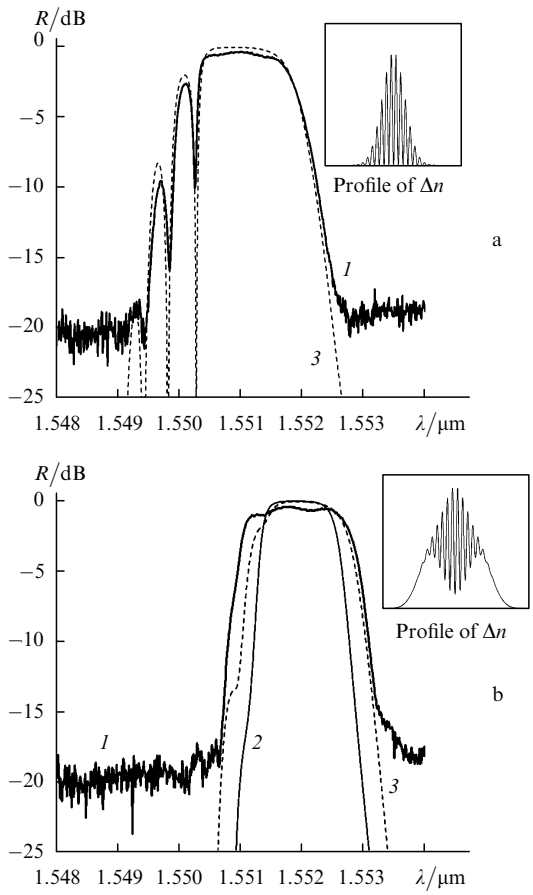

Figure 5. Spectra of the FBG (*1*) before (a) and after (b) the amplitude illumination and the results of numerical simulations of the spectrum of the FBG described by expression (6) for $w = 1$ mm, $s = 0.75$, $n_0\Lambda = 0.7748$ μm, $\Delta n_0 = \Delta n_{1,2} = 1.6 \times 10^{-3}$ for the symmetric amplitude illumination for $z_1 = z_2 = 1$ mm (*2*) and asymmetric amplitude illumination for $z_1 = 0.8$ μm and $z_2 = 1.2$ mm (*3*).

(8). Because the phase and amplitude of the wave solution of (7) are determined with an accuracy to a constant shift and a constant factor, respectively, the complex amplitude A_2 is arbitrary and was specified in the form

$$A_2 = (1, 0). \tag{9}$$

The coefficient K_c was determined from expression $K_c = 1/|\tilde{A}_1|$, where $\tilde{A}_1$ is the incident wave amplitude found by solving Eqn (7) under condition (8).

Equation (7) was solved by two numerical methods: the T-matrix method (see, for example, [10]) and the fourth-order Runge–Kutta method [11]. In the T-matrix method, the distribution of the refractive index $n(z)$ was approximated by a step function. The exact solution on each step is known and can be written in the form

$$E = A_j \exp(\mathrm{i}k_j z) + B_j \exp(-\mathrm{i}k_j z),$$

where j is the step number; A_j and B_j are the complex wave amplitudes; $k_j = k_0 n_j$; and n_j is the refractive index on the jth step. Between the adjacent steps the continuity conditions for the function E and its first derivative are specified. The method is exact if $n(z)$ is a step function; if $n(z)$ is a smooth function, the accuracy order coincides with the approximation order of the function $n(z)$.

Numerical calculations were performed by using programs placed at our disposal by the authors of paper [12], in which the amplitude and phase of the reflection coefficient and the group delay were calculated for a medium with the given inhomogeneous distribution of the refractive index. The input data for the programs (values of the coordinate in increasing order and the corresponding values of the refractive coefficient) were specified in the Mathematica program. The convergence of the numerical procedure was tested by determining the optimal length of the grating (integration region) and the optimal calculation step. The sufficient length for a grating with a Gaussian refractive index profile was $4w$; as the grating length was further increased, the difference from the previous result of calculations was less than −30 dB (less than the sensitivity limit of our experimental setup). The optimal calculation step proved to be equal to 0.075 μm; as the step was further decreased, the difference from the previous result was also less than −30 dB.

First we calculated the spectrum of the FBG with the Gaussian refractive index profile (4). Simulations performed for the reflection coefficient $R \sim 1$ gave the following dependences.

As the parameter Δn_0 increases, the width and amplitude of the main peak also increase, the side resonances grow in amplitude, and the number of resonances with the relative amplitude above −20 dB increases correspondingly, the distance between the resonances being virtually invariable. As a result, as the modulation amplitude of the refractive index is increased at a constant width of the Gaussian distribution, the effective interferometer base does not change, but the width of the spectrum increases in accordance with estimate (3). The results of simulations are in

good agreement with experimental FBG spectra (Figs 2 and 3).

As the radius w is increased at a constant Δn_0, the width and amplitude of the main resonance change weaker than with increasing Δn_0, but the distance between side resonances decreases and the number of resonances with the amplitude above -20 dB correspondingly increases. This is qualitatively explained by the fact that the interferometer base increases with increasing w, which results in a decrease in the distance between the resonances. A comparison of the experimental curves (and corresponding calculated curves) with close values of the induced refractive index but considerably different grating lengths (cf. Figs 2b and 3a) clearly demonstrates the decrease in the interval between zeroes of the reflection coefficient with increasing the grating length.

As the visibility s of the interference pattern increases, the modulation depth of the refractive index increases. This is manifested in the increase in the intensity and width of the main peak and side resonances.

To calculate the FBG apodized by exposing it to a Gaussian beam, we used expression (6). The simulation showed that the best suppression of side resonances was observed when the amplitudes of the modulated and homogeneous Gaussian components were close ($\Delta n_0 \approx \Delta n_1 \approx \Delta n_2$) and the illumination was symmetric with the displacement approximately equal to the beam radius ($z_1 \approx z_2 \approx w$).

The numerical analysis of the sensitivity of the shape of the spectrum to the deviation of parameters from their optimal values showed that the side resonances became noticeable when the displacements $z_{1,2}$ were smaller than the optimal value, $z_1 \approx z_2 < w$. A simultaneous decrease in the amplitude of the homogeneous illumination results in a similar effect, $\Delta n_1 \approx \Delta n_2 < n_0$. The width of the main resonance changes weakly in both these cases. Note that a change of only one of the parameters $z_{2,1}$, when another is close to the optimal value $z_{1,2} \approx w$ (and similarly for $\Delta n_{1,2} \approx \Delta n_0$) does not result in a strong increase in the side resonance amplitude, but the main resonance broadens considerably.

A comparison of experimental data obtained with the additional homogeneous illumination (Fig. 5b) with numerical calculations with parameters corresponding approximately to the optimal values realised in experiments shows that illumination suppresses side resonances down to the level below -20 dB, both in the theory and experiment. In this case, the position of the main resonance in the experiment corresponds to the calculated value, but its width somewhat exceeds the theoretical value [Fig. 5b, curve (*2*)]. A small displacement asymmetry $z_2 - z_1 \sim 0.4$ mm (which is possible in real experiments) taken into account in calculations results in the broadening of the resonance [curve (*3*) in Fig. 5] almost to its complete coincidence with the experimental spectrum.

5. Conclusions

The theoretical substantiation and experimental realisation of the method for FBG apodization proposed in our paper have shown that highly reflecting FBGs with side resonances suppressed down to the level below -20 dB can be easily written by a Gaussian laser beam. The method is based on the illumination of an optical fibre (with a FBG with a Gaussian profile of the induced refractive index preliminary written in it) by a homogeneous Gaussian beam on both sides from the FBG centre with the displacement approximately equal to the Gaussian beam radius. This results in the refractive index flattening and elimination of the effective resonator responsible for side resonances in the short-wavelength region of the FBG spectrum. The numerical simulation of the FBG spectrum with a Gaussian profile has demonstrated good agreement with experiments. The optimal parameters of additional illumination have been found and the sensitivity of the shape of the spectrum to the deviations of parameters from their optimal values has been analysed.

Acknowledgements. The authors thank O.V. Belai for his help in numerical calculations and D.V. Churkin for his help in experiments. This work was supported by the Ministry of Education and Science of the Russian Federation (Project Nos NSh-7214.2006.2 and 2006-RI-19.0/0012/644), programs of the Presidium and DPS, RAS, and integration projects of SB, RAS (3.11; 31).

References

1. Kashyap R. *Fiber Bragg Gratings* (San Diego: Acad. Press, 1999).
2. Vasil'ev S.A., Medvedkov O.I., Korolev I.G., Bozhkov A.S., Kurkov A.S., Dianov E.M. *Kvantovaya Elektron.*, **35**, 1085 (2005) [*Quantum Electron.*, **35**, 1085 (2005)].
3. Meltz G., Morey W.W., Glenn W.H. *Opt. Lett.*, **14**, 823 (1989).
4. Lemaire P.J., Atkins R.M., Mizrahi V., Reed W.A. *Electron. Lett.*, **29**, 1191 (1993).
5. Erdogan T. *J. Lightwave Technol.*, **15**, 1277 (1997).
6. Othonos A., Kalli K. *Fiber Bragg Gratings: Fundamentals and Aplications in Telecommunications and Sensing* (Norwood: Artech Hous, 1999).
7. Mizrahi V., Sipe J.E. *J. Lighywave Technol.*, **11**, 1513 (1993).
8. Abdullina S.R., Babin S.A., Vlasov A.A., Kablukov S.I. *Kvantovaya Elektron.*, **35**, 857 (2005) [*Quantum Electron.*, **35**, 857 (2005)].
9. Yariv A., Yeh P. *Optical Waves in Crystals: Propagation and Control of Laser Radiation* (New York: Wiley, 1984; Moscow: Mir, 1987).
10. Kotkin G.L., Tkachenko O.A., Tkachenko V.A. *Laboratornye raboty po kvantovoi mekhanike* (Laboratory Works on Quantum Mechanics) (Novosibirsk: Novosibirsk State University, 1987).
11. Kamke E. *Gewöhnliche Differentialgleichungen* (Leipzig: Acad. Verlag, 1959; Moscow: Nauka, 1965).
12. Belai O.V., Podivilov E.V., Shapiro D.A. *Opt. Commun.* (2006) (in press).